HHS Public Access

Author manuscript

Immunol Cell Biol. Author manuscript; available in PMC 2013 September 01.

Published in final edited form as:

Immunol Cell Biol. 2013 March ; 91(3): 195–200. doi:10.1038/icb.2013.1.

Differential modulation of experimental autoimmune encephalomyelitis by α9*- and β2*-nicotinic acetylcholine receptors

Alain R. Simard[1,2], **Yan Gan**[3], **Stéphanie St-Pierre**[1], **Ariana Kousari**[3], **Varun Patel**[3], **Paul Whiteaker**[4], **Barbara J. Morley**[5], **Ronald J. Lukas**[4], and **Fu-Dong Shi**[3]

[1]Département de Chimie et Biochimie, Université de Moncton, Moncton, NB, Canada

[2]Centre de Formation Médicale du Nouveau-Brunswick, Moncton, NB, Canada

[3]Division of Neurology, Barrow Neurological Institute, Phoenix, AZ, USA

[4]Division of Neurobiology, Barrow Neurological Institute, Phoenix, AZ, USA

[5]Boys Town National Research Hospital, Omaha, NE, USA

Abstract

Nicotine is a potent inhibitor of the immune response and is protective against experimental autoimmune encephalomyelitis (EAE). Initial studies suggested that the cholinergic system modulates inflammation via the α7-nicotinic acetylcholine receptor (nAChR) subtype. We recently have shown that effector T cells and myeloid cells constitutively express mRNAs encoding nAChR α9 and β2 subunits and found evidence for immune system roles for non-α7-nAChRs. In the present study, we assessed the effects of nAChR α9 or β2 subunit gene deletion on EAE onset and severity, with or without nicotine treatment. We report again that disease onset is delayed and severity is attenuated in nicotine-treated, wild-type mice, an effect that also is observed in α9 subunit knock-out (KO) mice irrespective of nicotine treatment. On the other hand, β2 KO mice fail to recover from peak measures of disease severity regardless of nicotine treatment, despite retaining sensitivity to nicotine's attenuation of disease severity. Prior to disease onset, we found significantly less reactive oxygen species production in the CNS of β2 KO mice, elevated proportions of CNS myeloid cells but decreased ratios of CNS macrophages/microglia in α9 or β2 KO mice, and some changes in iNOS, TNF-α and IL-1β mRNA levels in α9 KO and/or β2 KO mice. Our data thus suggest that β2*- and α9*-nAChRs, in addition to α7-nAChRs, play different roles in endogenous and nicotine-dependent modulation of immune functions and could be exploited as therapeutic targets to modulate inflammation and autoimmunity.

Corresponding Author: Alain Simard, Département de Chimie et Biochimie, Université de Moncton, Moncton, NB, CanadaE1A3E9, alain.simard@umoncton.ca, Phone : 1-506-858-4748, Fax : 1-506-858-4541.

The authors declare no conflict of interest.

Keywords

auto-immunity; cholinergic anti-inflammatory pathway; experimental autoimmune encephalomyelitis; inflammation; multiple sclerosis; nicotinic acetylcholine receptors

Introduction

Nicotinic acetylcholine receptor (nAChR) signalling is thought to have beneficial, natural, immunosuppressive consequences via what is called the cholinergic anti-inflammatory pathway (reviewed in (1)). Recent studies, including our own, have shown that exposure to nicotine significantly delays the onset and markedly attenuates the severity of disease symptoms in experimental autoimmune encephalomyelitis (EAE), a mouse model for multiple sclerosis (2–4). Nicotine appears to confer protection against EAE by modulating multiple immune functions, such as the production of inflammatory mediators and cell recruitment (1–4).

Early studies suggested that the cholinergic anti-inflammatory pathway acts via α7-nAChRs (5,6). However, our recent data demonstrated that nicotine may also act via other nAChR subtypes, since the drug retains the ability to modulate multiple immunological functions in nAChR α7 subunit knock-out (KO) mice (4). In addition, many immune cell types express mRNA for multiple nAChR subunits (7–10). In particular, nAChR α9 and β2 subunits are expressed in $CD4^+$ and $CD8^+$ T cells, monocytes, dendritic cells and microglia (4). However, whether α9*- or β2*-nAChRs (where the * indicates that additional nAChR subunits are known or possible assembly partners with the subunits specified (11)) are involved in the cholinergic anti-inflammatory pathway is unclear. To test for roles of α9*- and β2*-nAChRs, and mindful of the fact that nicotine is an agonist at most nAChR subtypes but is an antagonist at α9*-nAChRs (12), we assessed the ability of nicotine to modulate EAE onset and severity in nAChR α9 KO or β2 KO mice.

Results

Our previous studies showed that non-α7-nAChRs also may be involved in nicotine's protective effects against EAE onset and severity, and that many immune cells constitutively express nAChR α9 and β2 subunits (4). To determine if α9*-nAChRs also play a role in the protective cholinergic anti-inflammatory pathway, wild-type (WT) or nAChR α9 KO mice were immunized with $MOG_{35–55}$ on day 0 (4) and treated with phosphate-buffered saline (PBS) or nicotine (13 mg/kg/day of free base) from Days 0 to 28 (Figure 1A and B). The average of time of EAE onset (± S.E.M.) relative to the time of immunization was 8.7 ± 0.9 days in PBS-treated WT mice (WT + PBS) and 15.7 ± 3.3 days in nicotine-treated WT mice (WT + Nic), whereas the average maximum clinical score in WT + PBS mice was 2.7 ± 0.2 and 1.7 ± 0.5 in WT + Nic mice (all n=6, $p<0.05$). Therefore, nicotine once again delayed EAE onset and attenuated disease severity in WT mice. Interestingly, disease onset was delayed (14.5 ± 2.0 days in α9 KO + PBS mice, n=6, and 15.6 ± 1.7 days in α9 KO + Nic mice, n=7) and maximum clinical score was reduced (1.9 ± 0.3 in α9 KO + PBS mice and 1.9 ± 0.4 in α9 KO + Nic mice) in α9 KO mice (n = 6 per group), regardless of drug treatment ($p<0.05$ for α9 KO + Nic or α9 KO + PBS vs. WT + PBS mice), whereas no

additional nicotine effect was observed ($p>0.05$ for α9 KO + Nic vs. α9 KO + PBS mice). All animals recovered similarly from EAE to a terminal score of 0.5 to 0.7. These data suggest that α9*-nAChRs play roles in endogenous mechanisms that govern disease initiation and severity in EAE.

To assess the role of β2*-nAChRs in the cholinergic anti-inflammatory pathway, WT or β2 KO mice were immunized with $MOG_{35–55}$ on Day 0 and treated with PBS or nicotine from days 7 to 14 (Figure 1C and D). The timing difference for nicotine treatment in β2 KO as opposed to α9 KO mouse studies was influenced by osmotic minipump availability when animals were at the appropriate age for experimentation, but our previous studies showed that nicotine treatment starting at day 7 or at day 0 is equally effective in reducing disease severity (2). As expected, nicotine treatment attenuated peak clinical scores (2.2 ± 0.2 in WT + PBS vs. 1.1 ± 0.3 in WT + Nic mice, $p<0.05$) in WT mice, and there was delayed onset of symptoms (9.6 ± 0.2 days in WT + PBS vs. 12.0 ± 0.5 days in WT + Nic mice, $p<0.05$, n = 6 per group). In β2 KO mice, nicotine did not have a significant effect on disease onset (10.1 ± 0. 7 days in β2 KO + PBS compared to 11.6 ± 1.6 days in β2 KO + Nic mice, $p>0.05$, n = 6 per group), but it did attenuate maximum clinical score (2.4 ± 0.1 in β2 KO + PBS vs 1.7 ± 0.3 in β2 KO + Nic, $p<0.05$). Interestingly, none of the β2 KO mice recovered from disease (Terminal Score of 1.9 ± 0.2 in β2 KO + PBS and 1.4 ± 0.4 in β2 KO + Nic mice) to the same extent as WT mice (Terminal Score of 0.7 ± 0.2 in WT + PBS and 0.6 ± 0.2 in WT + Nic mice), an effect that reached statistical significance ($p<0.05$, β2 KO vs. WT mice). Altogether, these data suggest that β2*-nAChRs are important for natural recovery from EAE but are not involved in nicotine's protective effects against EAE onset and severity.

Due to these striking results, we assessed if the lack of recovery in β2 KO mice could be explained by a difference in CNS inflammation. Luminol is a compound that emits blue luminescence when exposed to reactive oxygen species (ROS) and thus can be used to quantify general inflammation in vivo (13). Bioluminescence imaging revealed that luminescence was significantly lower in β2 KO EAE mice than in their WT EAE counterparts at day 7 post-immunization (10,000 ± 2,300 in WT vs 3,600 ± 1,100 in β2 KO mice, $p<0.05$, n = 5 per group), whereas no differences were observed at later time points (Figure 1E). These results suggest that β2*-nAChRs may be involved in endogenous mechanisms that regulate early stages of inflammation.

One of the key events that is crucial for disease onset is the infiltration of inflammatory cells to the CNS. Nicotine treatment was previously shown to reduce the numbers of myeloid cells in the CNS of EAE mice (4). We thus assessed the proportions of macrophages and microglial cells, based on flow cytometric analysis of CD11b and CD45 expression, in the CNS of WT (n = 6), α9 KO mice (n = 4) or β2 KO mice (n = 5) on day 7 post-EAE immunization, which is the day prior to with disease onset in WT EAE mice (Figure 1A). In WT EAE mice, 12.4 ± 1.8 % of total CNS cells were $CD11b^{+}/CD45^{+}$, while this number increased to 23.9 ± 1.1 % in α9 KO or to 21.3 + 1.0 % in β2 KO EAE mice ($p<0.001$ vs WT; Figure 2A). This shows that the proportion of CNS myeloid cells increases in α9 KO or β2 KO EAE mice. We extended this analysis to discriminate microglia ($CD11b^{+}/CD45^{med}$) and infiltrating macrophages/activated microglia ($CD11b^{+}/CD45^{high}$) (14). Microglia accounted for 2.4 ± 0.5% of total CNS cells in WT EAE mice but their levels were

significantly increased to 9.0 ± 1.4% in α9 KO and 14.2 ± 1.2% in β2 KO ($p<0.001$ vs WT) EAE mice (Figure 2A,B). Interestingly, the percentage of CNS myeloid cells that were macrophages/activated microglia increased from 10.0 ± 1.6 % in WT to 14.9 ± 1.2 % in α9 KO EAE mice ($p<0.05$ vs WT), while it decreased slightly but not significantly to 7.1 ± 0.5 % in β2 KO EAE mice ($p=0.07$ vs WT). Thus, the percentage of infiltrating macrophages/activated microglia as a proportion of CNS myeloid cells was 80.6% in WT EAE mice, 62.3% in α9 KO EAE mice ($p<0.05$ vs WT mice) and 33.3 ± 2.9 % in β2 KO EAE mice ($p<0.001$ vs WT mice). To the contrary, the percentage of CNS $CD11b^+/CD45^+$ cells that are microglia was 19.4 ± 4.1 % in WT EAE mice, 37.7 ± 4.8 % in α9 KO EAE mice ($p<0.01$ vs WT) and 66.7 ± 2.8 % in β2 KO EAE mice ($p<0.001$ vs WT). The ratio of infiltrating macrophages/activated microglia to microglia is significantly decreased in α9 KO (1.70) and β2 KO (0.53) compared to WT (4.13) EAE mice ($p<0.05$ and $p<0.001$, respectively, vs WT mice). There is a formal possibility that the results could be alternatively explained by 16–18% decreases in percentages of glial and neuronal populations if leukocyte populations actually held steady in α9 or β2 KO EAE mice, which would suggest a substantial, and equally significant, effect of nAChR elimination. However, we favor the interpretation that genetic deletion of the α9 nAChR and β2 nAChR subunits has a substantial impact on ratios (and, presumably, absolute numbers) of microglia and infiltrating macrophages/activated microglia in the CNS of EAE mice.

We next determined if mRNA levels for iNOS, TNF-α and IL-1β were modified in the brain and spinal cord of α9 KO or β2 KO EAE mice at day 7 post-immunization (Figure 2C). Relative to WT EAE mice, transcript levels for these pro-inflammatory markers were unchanged in the brains of α9 KO or β2 KO EAE mice. On the other hand, mRNA levels for iNOS in the spinal cord were 73 ± 17% in α9 KO and 64 ± 21% in β2 KO EAE mice compared to their levels in WT EAE mice ($p<0.05$), supporting the lower Luminol bioluminescence in the brain of β2 KO EAE mice at the same time point. TNF-α mRNA levels in the spinal cord were 1.75 ± 0.45 times those in WT EAE mice when assessed in β2 KO EAE mice ($p<0.05$) but were unchanged in α9 KO EAE mice. However, spinal cord IL-1β mRNA levels were 55 ± 18% of those in WT EAE mice when measured in α9 KO EAE mice ($p<0.05$) but unchanged in β2 KO EAE mice. α9*- and β2*-nAChRS therefore differentially modulate iNOS, IL-1β and TNF-α production.

Discussion

α7-nAChRs were the first suggested to be involved in the cholinergic anti-inflammatory pathway (5,6). α7-nAChR elimination by gene deletion abolishes nicotine's protection against EAE, implicating them in nicotine-dependent protection (3,4). However, these studies also show that α7 KO mice still develop EAE and recover as do wild-type animals in the absence of drug treatment, suggesting that α7-nAChRs are not key players in endogenous nAChR-dependent immunoregulatory processes in the EAE model. Moreover, we also recently demonstrated that roles of nAChRs in immunoregulation may be more complex than previously thought (4), and the current study expands on those findings.

The first interesting observation in this study is that α9 subunit gene deletion alone delays the onset and reduces the severity of EAE. These findings suggest that α9*-nAChRs are

naturally involved in endogenous pro-inflammatory mechanisms required for disease initiation and evolution, likely via the endogenous agonist, acetylcholine. We also found that nicotine exposure has no observable effect in α9 KO mice. That is, nicotine treatment of WT mice and α9*-nAChR elimination have the same effect. This is not surprising given that nicotine is an antagonist of α9*-nAChRs, contrary to acetylcholine (12). These new findings, in addition to previous reports demonstrating the beneficial role of α7-nAChRs (3,4), suggest that antagonism of α9*- and activation of α7-nAChRs are both required for nicotinic protection against EAE onset, although their effects do not appear to be additive.

Peripheral monocyte/macrophage recruitment, microglial activation, iNOS upregulation and pro-inflammatory cytokine production are all important mechanisms for EAE initiation and can also dictate disease severity (15–17). Interestingly, our results show that although the proportions of $CD11b^+/CD45^+$ cells increase in the CNS of α9 KO EAE mice compared to their WT counterparts, there is a more balanced ratio of infiltrating macrophages/activated microglia to microglia in α9 KO EAE mice (1.65 : 1) than in WT EAE mice (4.15 : 1), providing a possible mechanism for protection against EAE. In addition, we found that mRNA levels for iNOS and IL-1β were lower in α9 KO than in WT EAE mice. These findings suggest that even though proportions of microglia and macrophages are increased, there is a reduced production of at least some pro-inflammatory mediators in the CNS of α9 KO EAE mice, which may also explain the lower EAE severity and delayed disease onset observed in these mice. Importantly, these effects were observed in the absence of nicotine. Our data therefore indicate that α9*-nAChRs may play an endogenous role in the regulation of macrophage recruitment and inflammation, the combination of which ameliorates disease progression. In addition, the fact that genetic deletion of the α9 nAChR subunit protects against disease and some of its pathological mechanisms also suggests that endogenous activation of α9*-nAChRs may have pro-inflammatory consequences, rather than the anti-inflammatory effects normally observed after nicotine binding to α7-nAChRs (2–4).

Our new findings also show that nicotine retains the ability to diminish the severity of EAE symptoms in β2 KO mice. This indicates that β2*-nAChRs are not involved in nicotine-dependent protection against EAE, at least not at the doses used and in nicotine's effects on early or mid-disease progression. Of equal or perhaps greater importance is the striking observation that recovery is prevented in β2 KO mice, regardless of drug treatments. This finding suggests that nAChR signalling via β2*-nAChRs is important for mechanisms of repair. Curiously, we found that measures of CNS inflammation based on levels of ROS in the brain and iNOS expression in the spinal cord are significantly reduced at day 7 post-immunization, which is immediately prior to the emergence of disease signs, in β2 KO mice. Technical matters in luminescence imaging protocols may have compromised the ability to detect changes in ROS production in the spinal cord or may have enhanced such detection in surface meninges in the brain in β2 KO EAE mice, and there are mixed effects in β2 KO EAE mice on mRNA levels examined that relate to inflammatory processes (increased TNF-α, unaltered IL-1β, lowered iNOS, but only in spinal cord and not in brain). Nevertheless, even though proportions of CNS myeloid cells were increased in these animals, they have more microglia than infiltrating macrophages/activated microglia. Although infiltrating macrophages are important for disease initiation, they also are crucial for myelin debris clearance and repair mechanisms (18), meaning that reduction in their numbers could

correlate with the compromised recovery observed in β2 KO EAE mice. Alternatively or perhaps in addition, the increased TNF-α production observed in the spinal cord could lead to more extensive cell death and a prolonged inflammatory response in β2 KO EAE mice. More experiments will be necessary to test these hypotheses.

Overall, these data demonstrate that several nAChR subtypes are involved, albeit differently, in the cholinergic anti-inflammatory pathway, both naturally and in response to nicotine. More importantly, our data suggest that each nAChR subtype may modulate unique cellular immune functions. Mechanisms that can explain our observations remain to be determined, and more experiments are required in order to fully understand the complexities of the cholinergic anti-inflammatory pathway. However, our findings raise the possibility of using nAChR subtype-selective compounds to modulate specific immune functions for the treatment of inflammatory diseases, especially at different stages in disease progression or recovery. More specifically, we suggest that early inhibition of α9*-nAChR function and later activation of β2*-nAChRs could be beneficial in treatment of multiple sclerosis or other immunological disorders.

Methods

Mice

B6 (H-2^b) mice were purchased from Taconic (Germantown, NY, USA). The nAChR α9 KO mouse model was generated by the deletion of exons 1 and 2 containing the translation/transcription initiation sites, and confirmed by Southern blotting (Genoway, Inc). The knock-out line was subsequently backcrossed at the Boys Town National Research Hospital (BTNRH) to B6 mice (Jackson Laboratory) using Marker-Assisted Accelerated Backcrossing (MAX BAX; Charles River) until 99.8–100% congenicity was achieved. The absence of α9 subunit transcript in the constitutive knock-out was verified by PCR and qPCR employing a custom PCR Array (Qiagen) and using samples from wild-type mouse cochlear tissue as the positive control. In cochlear tissue, there is no change in any of the other nAChR subunits, indicating that there is no nAChR subunit compensation for the loss of α9 subunits, and α9 KO mice have the expected cochlear phenotype of aberrant innervation of hair cells (19). The α9 KO mice used in this study were bred at BTNRH and shipped to the Barrow Neurological Institute (BNI) at weaning, where they were maintained until use. nAChR β2 subunit knock-out mice, backcrossed to the B6 background for more than 11 generations, were originally provided by Marina Picciotto (Yale University, New Haven, CT, USA) and bred at the BNI. All animals were housed in pathogen-free animal facilities. Female mice used were 7 to 8 weeks of age at the experiment's inception. Experiments were reviewed, approved and conducted in accordance with institutional and NIH guidelines.

Induction of acute EAE

Mice were immunized with $MOG_{35–55}$ as done previously (4). Briefly, mice were injected subcutaneously (s.c.) in the hind flank with 200 μg of $MOG_{35–55}$ peptide (single letter amino acid sequence; M-E-V-G-W-Y-R-S-P-F-S-R-V-V-H-L-Y-R-N-G-K; Bio Synthesis Inc., Lewisville, TX, USA) in complete Freund's adjuvant (CFA) (Difco, Detroit, MI, USA)

containing 500 μg of non-viable, desiccated *Mycobacterium tuberculosis*. On the day of and 2 days after immunization, the mice also were inoculated with 200 ng of pertussis toxin (List Biologic, Campbell, CA, USA) intraperitoneally (i.p.). Mice were monitored daily for symptoms scored on an arbitrary scale of 0 to 5 with 0.5 increments: 0, no symptoms; 1, flaccid tail; 2, hind limb weakness or abnormal gait; 3, complete hind limb paralysis; 4, complete hind limb paralysis with forelimb weakness or paralysis; 5, moribund or deceased.

Nicotine treatment

(−)Nicotine bitartrate (Sigma-Aldrich, St. Louis, MO, USA) in phosphate-buffered saline (PBS) or a solution containing PBS alone was freshly prepared and loaded into Alzet® osmotic minipumps (models 1007D or 1004, Durect Corporation, Cupertino, CA, USA) 24 h before pump implantation, as done previously (4). The pumps were implanted subcutaneously on the right side of the back of the mouse and continuously delivered either PBS or nicotine salt at ~13 mg of nicotine free base/kg/d for either 7 days (β2 study, starting on day 7 post-immunization) or 28 days (α9 study, starting on day of immunization), and then the pumps were removed.

In vivo CNS bioluminescence

For imaging of reactive oxygen species generation in brain, bioluminescence images in live mice were captured using the Xenogen IVIS200 imager (Caliper Life Sciences, Hopkinton, MA) 20 minutes after i.p. injection of 0.1 ml of 50 mg/ml Luminol Sodium Salt (Sigma-Aldrich, St. Louis, MO, USA). A region of interest (ROI) tool was used to measure luminescence intensity. Data were collected as photons/sec/cm^2 using the Living Image® software (Caliper Life Sciences, Hopkinton, MA).

Flow cytometry

Mice were sacrificed at day 7 after EAE induction, and perfused with PBS delivered transcardially to eliminate contaminating blood cells in the CNS. Brains and spinal cords were removed, halved, more finely dissected, subjected to enzymatic digestion, and processed to remove myelin and other debris on Percoll density gradients, yielding a mixture of leukocytes, neurons and glia in the cell pellet, as described (20). Cells were resuspended and stained for myeloid cell surface markers CD11b and CD45 (targeted by the indicated antibody fluorescently tagged with either FITC, PE, allophycocyanin, PE-Cy5 or PE-Cy7), as described (4). Appropriate isotype controls were always included. CD45 and CD11b expression were analysed on live cells only by first gating for live leukocytes and other neuronal or glial cells of similar granularity and size as determined by their FSC/SSC properties. All samples were analyzed on a FACSAria™ using Diva.

qRT-PCR

The remaining half of the brains and spinal cords, obtained as described above, were used for qRT-PCR. To this end, tissues were homogenized with a glass homogenizer, and total RNA was purified with the Trizol Plus RNA Purification System (Invitrogen), as per the supplied protocol. cDNA was then generated using the SuperScript III First Strand cDNA Synthesis kit (Invitrogen) using Oligo-dT oligomers. qRT-PCR was then performed on the

CFX96 Real-time PCR Detection System (BioRad), using SsoAdvanced™ SYBR® Green Supermix (Bio-Rad)and the following primers: mouse GAPDH sense 5′-AGCCTCGTCCCGTAGACAA-3′ and anti-sense 5′-ATGAAGGGGTCGTTGATGGC-3′ mouse iNOS sense 5′-GGCAGCCTGTGAGACCTTTG-3′ and anti-sense 5′-GCATTGGAAGTGAAGCGTTTC-3′; mouse TNF-α sense 5′-CAAAATTCGAGTGACAAGCCTGTA-3′ and anti-sense 5′-CAGCTGCTCCTCCACTTGGT-3′; mouse IL-1β sense 5′-TGACGGACCCCAAAAGATGAA-3′ and anti-sense 5′-AGTGATACTGCCTGCCTGAAG-3′. Cycle conditions were: 95 C for 30 sec, followed by 40 cycles of 95 C for 5 sec and 58 C for 30 sec followed by a melt curve 65–95 C (0.5 increments) for 5 sec/step. Results were analyzed using CFX manager™ software.

Statistical analysis

Fisher's exact test or Mann-Whitney's U test were applied to analyze disease manifestation or severity, respectively. Student's *t*-tests were used to compare differences between two groups. Differences of three or more groups were evaluated by performing ANOVA. Results are always presented ± S.E.M.

Acknowledgments

We thank Pamela Bortz for technical assistance. This project was funded by the National Institutes of Health (R01AI083294 to F-D. Shi), the Barrow Neurological Foundation (to R.J. Lukas and to F-D. Shi), the Multiple Sclerosis Society of Canada (postdoctoral fellowship to A.R. Simard), the New Brunswick Innovation Foundation (to A.R. Simard), and the Nebraska Tobacco Settlement Biomedical Research Fund (to B.J. Morley).

References

1. Tracey KJ. Reflex control of immunity. Nature reviews. 2009 Jun; 9(6):418–28.
2. Shi FD, Piao WH, Kuo YP, Campagnolo DI, Vollmer TL, Lukas RJ. Nicotinic attenuation of central nervous system inflammation and autoimmunity. J Immunol. 2009 Feb 1; 182(3):1730–9. [PubMed: 19155522]
3. Nizri E, Irony-Tur-Sinai M, Lory O, Orr-Urtreger A, Lavi E, Brenner T. Activation of the cholinergic anti-inflammatory system by nicotine attenuates neuroinflammation via suppression of Th1 and Th17 responses. J Immunol. 2009 Nov 15; 183(10):6681–8. [PubMed: 19846875]
4. Hao J, Simard AR, Turner GH, Wu J, Whiteaker P, Lukas RJ, et al. Attenuation of CNS inflammatory responses by nicotine involves alpha7 and non-alpha7 nicotinic receptors. Experimental Neurology. 2011 Jan; 227(1):110–9. [PubMed: 20932827]
5. Wang H, Yu M, Ochani M, Amella CA, Tanovic M, Susarla S, et al. Nicotinic acetylcholine receptor alpha7 subunit is an essential regulator of inflammation. Nature. 2003 Jan 23; 421(6921): 384–8. [PubMed: 12508119]
6. Shytle RD, Mori T, Townsend K, Vendrame M, Sun N, Zeng J, et al. Cholinergic modulation of microglial activation by alpha 7 nicotinic receptors. Journal of Neurochemistry. 2004 Apr; 89(2): 337–43. [PubMed: 15056277]
7. Sato KZ, Fujii T, Watanabe Y, Yamada S, Ando T, Kazuko F, et al. Diversity of mRNA expression for muscarinic acetylcholine receptor subtypes and neuronal nicotinic acetylcholine receptor subunits in human mononuclear leukocytes and leukemic cell lines. Neuroscience Letters. 1999 Apr 30; 266(1):17–20. [PubMed: 10336173]
8. Matsunaga K, Klein TW, Friedman H, Yamamoto Y. Involvement of nicotinic acetylcholine receptors in suppression of antimicrobial activity and cytokine responses of alveolar macrophages to Legionella pneumophila infection by nicotine. J Immunol. 2001 Dec 1; 167(11):6518–24. [PubMed: 11714820]

9. Fujii T, Takada-Takatori Y, Kawashima K. Basic and clinical aspects of non-neuronal acetylcholine: expression of an independent, non-neuronal cholinergic system in lymphocytes and its clinical significance in immunotherapy. Journal of Pharmacological Sciences. 2008 Feb; 106(2): 186–92. [PubMed: 18285654]

10. Kawashima K, Yoshikawa K, Fujii YX, Moriwaki Y, Misawa H. Expression and function of genes encoding cholinergic components in murine immune cells. Life Sci. 2007 May 30; 80(24–25): 2314–9. [PubMed: 17383684]

11. Lukas RJ, Changeux JP, Le Novere N, Albuquerque EX, Balfour DJ, Berg DK, et al. International Union of Pharmacology. XX. Current status of the nomenclature for nicotinic acetylcholine receptors and their subunits. Pharmacol Rev. 1999 Jun; 51(2):397–401. [PubMed: 10353988]

12. Verbitsky M, Rothlin CV, Katz E, Elgoyhen AB. Mixed nicotinic-muscarinic properties of the alpha9 nicotinic cholinergic receptor. Neuropharmacology. 2000 Oct; 39(13):2515–2524. [PubMed: 11044723]

13. Gross S, Gammon ST, Moss BL, Rauch D, Harding J, Heinecke JW, et al. Bioluminescence imaging of myeloperoxidase activity in vivo. Nat Med. 2009 Apr; 15(4):455–461. [PubMed: 19305414]

14. Greter M, Heppner FL, Lemos MP, Odermatt BM, Goebels N, Laufer T, et al. Dendritic cells permit immune invasion of the CNS in an animal model of multiple sclerosis. Nat Med. 2005 Mar; 11(3):328–34. [PubMed: 15735653]

15. Ajami B, Bennett JL, Krieger C, McNagny KM, Rossi FM. Infiltrating monocytes trigger EAE progression, but do not contribute to the resident microglia pool. Nat Neurosci. 2011 Jul 31; 14(9): 1142–1149. [PubMed: 21804537]

16. Ding M, Zhang M, Wong JL, Rogers NE, Ignarro LJ, Voskuhl RR. Antisense knockdown of inducible nitric oxide synthase inhibits induction of experimental autoimmune encephalomyelitis in SJL/J mice. J Immunol. 1998 Mar 15; 160(6):2560–2564. [PubMed: 9510151]

17. Compston A, Coles A. Multiple sclerosis. Lancet. 2002 Apr 6; 359(9313):1221–1231. [PubMed: 11955556]

18. Barrette B, Hebert MA, Filali M, Lafortune K, Vallieres N, Gowing G, et al. Requirement of myeloid cells for axon regeneration. J Neurosci. 2008 Sep 17; 28(38):9363–9376. [PubMed: 18799670]

19. Morley B, Simmons D. Characterization of Nicotinic Acetylcholine Receptor Knockout. Proc of the Midwinter Res Mtng of the Am Otolarngol Assoc. 2012; 35:263.

20. Nikodemova M, Watters JJ. Efficient isolation of live microglia with preserved phenotypes from adult mouse brain. J Neuroinflammation. 2012 Jun 28.9:147. [PubMed: 22742584]

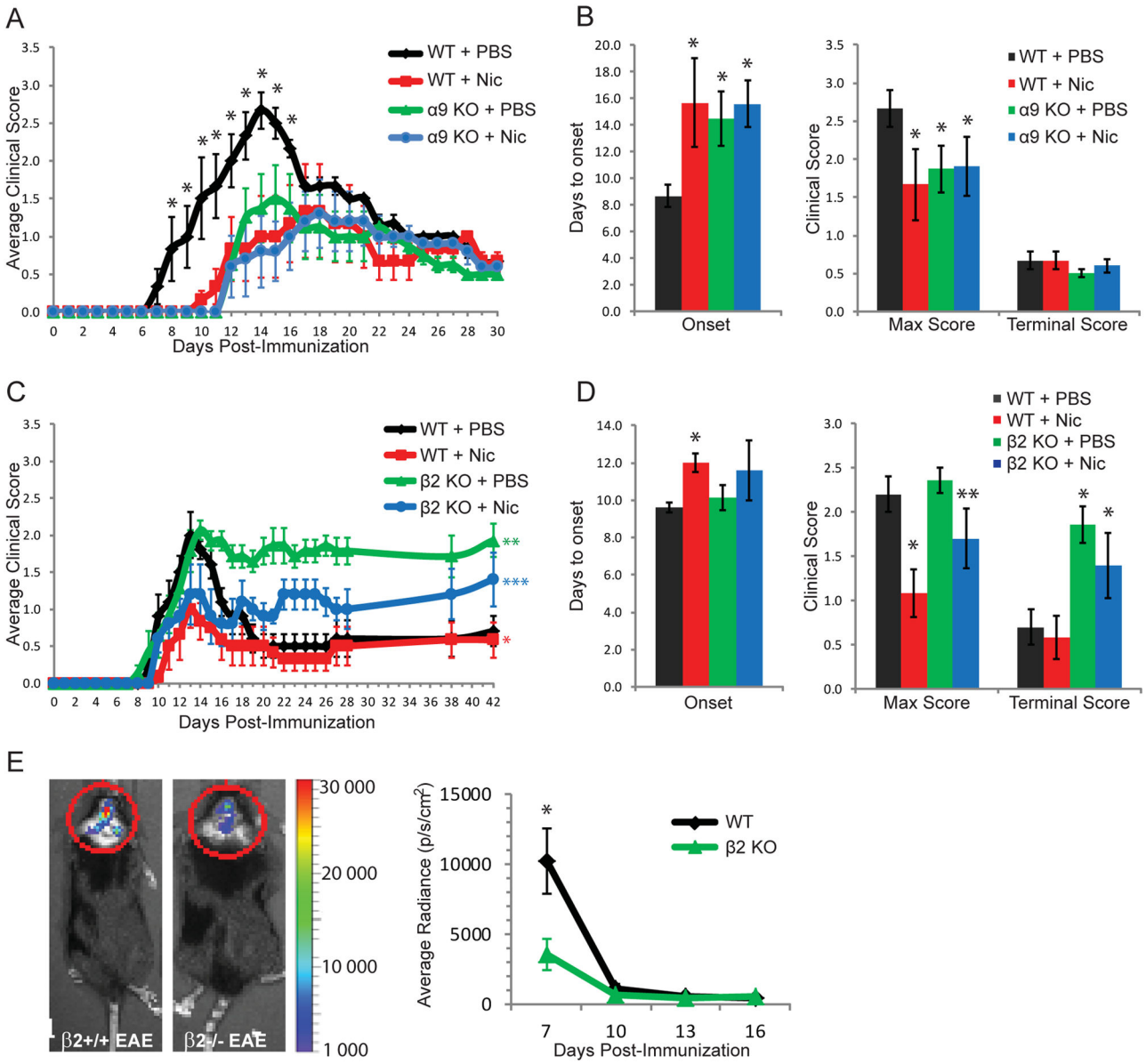

Figure 1. Clinical features of EAE in nicotine-treated, nAChR α9 and β2 subunit knock-out mice

A, Average clinical scores are shown as a function of days post-immunization for wild-type (WT) or nAChR α9 subunit knock-out (α9 KO) EAE mice treated with nicotine (Nic) or phosphate-buffered saline (PBS) subcutaneously, via mini-osmotic pumps, from day 0–30. * denotes $p<0.05$ vs. all other groups at days specified. **B,** Average number of days until the first appearance of clinical symptoms (Onset), the mean maximum clinical score (Max Score), and the average clinical score at day 30 (Terminal Score) are shown for the studies displayed in panel A. Whereas nicotine delayed the onset and reduced the severity of EAE in WT mice, as expected, this protection against disease was observed in α9 KO mice irrespective of Nic or PBS treatments. * indicates $p<0.05$ vs WT + PBS mice. **C,** Average clinical scores are shown at the indicated time post-immunization for WT or nAChR β2 subunit knock-out (β2 KO) EAE mice treated with nicotine or PBS from day 7–14. *

signifies $p<0.05$ for WT + Nic vs. WT + PBS mice at days 11–15; ** denotes $p<0.05$ for β2 KO + PBS vs. WT + PBS vs. WT Nic, or vs. β2 KO + Nic at days 16–42; *** indicates $p<0.05$ for β2 KO + Nic vs. WT + PBS or vs. WT + Nic at days 19–42. **D,** Onset, Max Score and Terminal Score results are shown for the studies described in panel C. * indicates $p<0.05$ vs WT + PBS, while ** denotes $p<0.05$ vs β2 KO + PBS. Nicotine thus delayed EAE onset and reduced disease severity in WT mice and reduced diseases severity in β2 KO mice. However, β2 KO EAE mice did not recover from disease, irrespective of nicotine or PBS treatments. **E,** In a separate set of experiments, Luminol was injected into WT or β2 KO EAE mice (no nicotine treatment), and in vivo bioluminescence in the brain was quantified on days 7, 10, 13 or 16 as a measure of CNS inflammation. Luminescence was significantly lower in β2 KO mice, as compared to WT mice, at day 7 post-immunization. * denotes $p<0.05$ between groups. Error bars represent S.E.M.

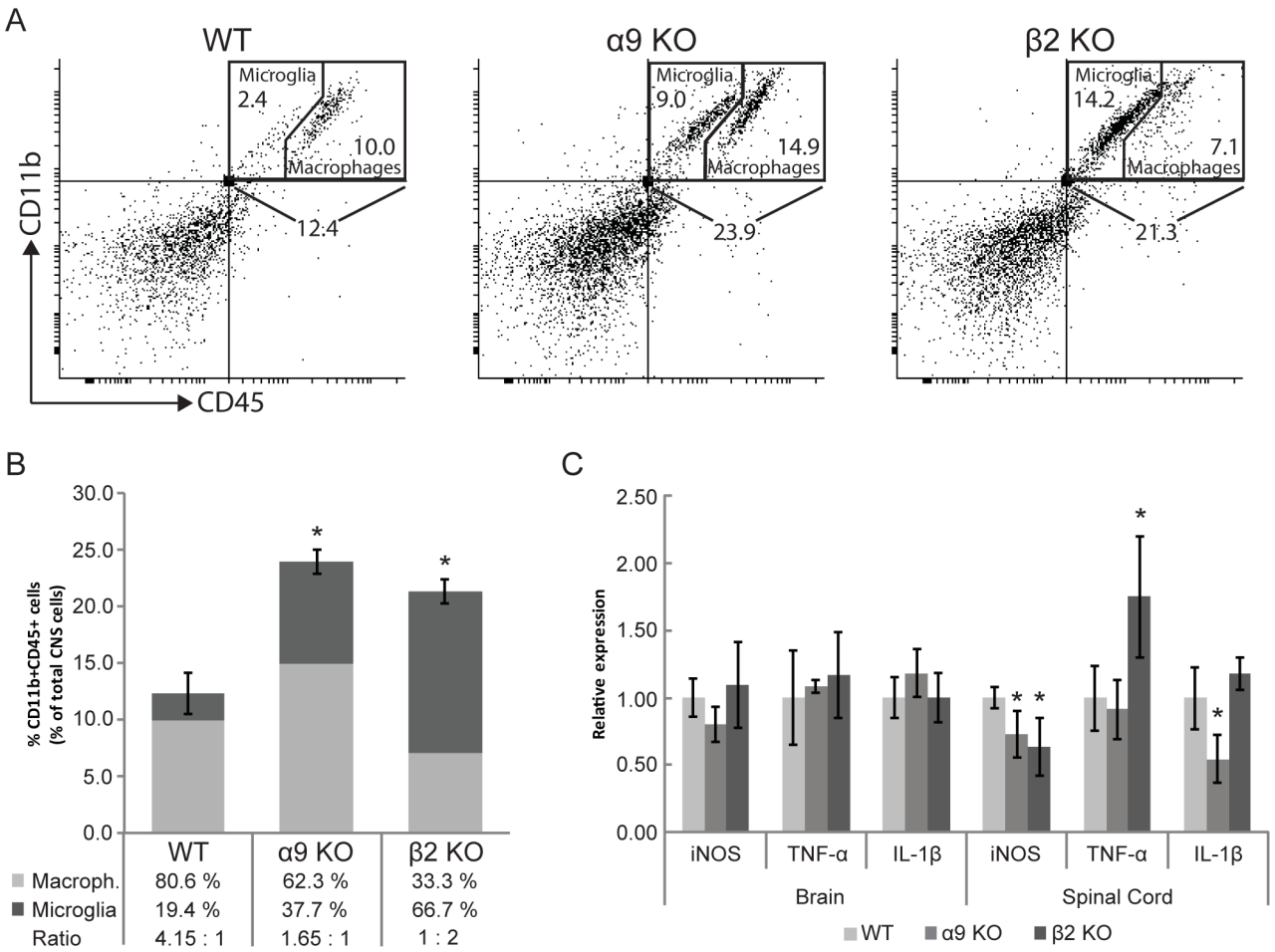

Figure 2. Myeloid cell numbers and cytokine production in the CNS of nAChR α9 or β2 subunit knock-out mice

WT, α9 KO or β2 KO mice were immunized with $MOG_{35–55}$ and sacrificed 7 days later. **A,** Myeloid cells ($CD11b^+/CD45^+$) within the entire population of brain and spinal cord cells were discriminated from other $CD11b^-/CD45^-$ leukocytes, neurons and glia by flow cytometry and further sub-divided into microglia ($CD11b^+/CD45^{med}$) or macrophage ($CD11b^+/CD45^{high}$) populations. **B**, Results are presented graphically for the percentages of myeloid cells relative to CNS cells and of ratios of infiltrating macrophages (light gray) to microglia (dark gray). Total myeloid cell numbers are increased, but ratios of infiltrating macrophages to microglia are significantly lower in the CNS of α9 KO or β2 KO EAE mice compared to in WT EAE mice. **C,** mRNA levels for the indicated genes in α9 KO or β2 KO EAE mice were assessed by qRT-PCR and are presented normalized to levels in WT EAE mice (*p<0.05). Error bars represent S.E.M.